



ORIGINAL ARTICLE

Calycosin-triblock copolymer nanomicelles attenuate doxorubicin-induced cardiotoxicity through upregulation of ERp57



Xiaoyan Wang, Lixiong Zeng, Shan Tu, Fei Ye, Zhihui Zhang*

Department of Cardiology, the Third Xiangya Hospital of Central South University, Changsha 410013, Hunan, China

Received 29 January 2021; accepted 23 March 2021

Available online 31 March 2021

KEYWORDS

Calycosin;
Triblock;
Nanomicelle;
Doxorubicin;
Cardiotoxicity;
ERp57 mRNA

Abstract It has been indicated that doxorubicin (Dox) can induce some unwanted cardiotoxicity through different signaling pathways. In the present study, calycosin-PEG-PPG-PEG copolymer nanomicelles were developed and well-characterized by different techniques. Afterwards, the protective effects of calycosin-triblock copolymer nanomicelles against Dox-stimulated cardiotoxicity in H9C2 cardiomyocytes were explored by viability, reactive oxygen species (ROS), and reactive nitrogen species (RNS) assays. Also, the expression of ERp57, p53, Bax, and Bcl-2 at both mRNA and protein levels were assessed by qPCR and western blot, respectively. It was seen that synthesized calycosin-triblock copolymer nanomicelles had a size of around 20–30 nm with good colloidal stability, sustained drug release and improved dissolution rate. Also, it was shown that calycosin-triblock copolymer nanomicelles can mitigate Dox-induced cardiotoxicity through a remarkable reduction in ROS and RNS generation. Also, it was found that calycosin-triblock copolymer nanomicelles resulted in the downregulation of Bax and p53 and overexpression of Bcl-2 and ERp57 at both mRNA and proteins levels and these protective effects were inhibited in the presence of ERp57-siRNA silencing. Therefore, this study may provide useful information about the development of drug-loaded nanomicelles for mitigation of Dox-induced toxicity.

© 2021 The Authors. Published by Elsevier B.V. on behalf of King Saud University. This is an open access article under the CC BY-NC-ND license (<http://creativecommons.org/licenses/by-nc-nd/4.0/>).

1. Introduction

Doxorubicin (Dox) is one of the most effective anti-cancer drugs in the treatment of malignant tumors (Tacar et al., 2013). However, clinical use of this drug causes some unwanted effects on cardiac, smooth, and skeletal muscle function (Hayward et al., 2013). The heart due to the high density of mitochondria and the need for more energy than other tissues, is known to be more sensitive to lipid peroxidation and induced Dox-induced programmed apoptosis (Kalyanaraman et al., 2002). Also, the lack of antioxidant enzymes required to detoxify dismutase anions and hydrogen peroxide in the heart tissue causes the

* Corresponding author at: NO. 138, tongzipo Road, Yuelu District, Changsha 410013, Hunan Province, China.

E-mail address: ZhihuiZhang.cardiac@yahoo.com (Z. Zhang).

Peer review under responsibility of King Saud University.



production and accumulation of free radicals, resulting in lipid ion peroxidation and extensive membrane degradation, endoplasmic reticulum and mitochondrial nucleic acid (Deres et al., 2005). This is while some findings show that the risk of cancer increases exponentially with age, so that cancer in the elderly is several times higher than reported in young people (Jones and Laird, 1999). In fact, the incidence of cancer, like other age-related erosive diseases, has increased dramatically among the elderly (Jones and Laird, 1999). Therefore, due to the harmful effects of doxorubicin treatment, especially in the case of cardiotoxicity, the need for diagnostic, preventive and therapeutic measures in this area is increasing (Zilinyi et al., 2018). Indeed, it has been reported that Dox-induced oxidative stress results in some significant changes in heart tissue, such as loss of fibers, intercellular edema, and damage to the mitochondria (Ascensão et al., 2006). Changes such as extensive degeneration, destruction of the mitochondrial cristae, and abnormal formation, shape, and size of heart tissue have been reported (Ascensão et al., 2006). Several anti-free radical agents, e.g., enzymes and drugs (McCord, 1986; Bernier et al., 1986; Martin et al., 2001; Hearse and Tosaki, 1987), spin traps (Tosaki and Braquet, 1990), plant extracts (Najafi et al., 2015; Bak et al., 2006), have been used to eliminate the harmful and injurious effects of ROS and RNS. Thus, the protection of cells and tissues against cellular damages is a crucial step to prevent necrotic, apoptotic, and autophagic cell deaths (Haines et al., 2013; Koleini and Kardami, 2017; Prathumsap et al., 2020).

Therefore, the use of potential antioxidants can be a promising approach for reducing the Dox-induced cardiotoxicity.

Calycosin as the major active component of *Radix astragali* has been reported to show different potential pharmaceutical features (Gao et al., 2014), including reduction of myocardial injury (Tsai et al., 2019; Liu et al., 2020), preservation of heart function (Martin et al., 2001), and reduction of infarct size and oxidative stress in cardiac cells (Huang et al., 2020). It has been also demonstrated that calycosin causes cardiovascular protective effects (Li et al., 2020) through activating estrogen receptor- α/β (Liu et al., 2016). However, calycosin due to its hydrophobic structure usually should be used in a high concentration which results in its poor colloidal stability and limited bioavailability (Deng et al., 2020).

In classical drug delivery systems, the drug is distributed aimlessly and generally throughout the body, and the cells take some of the drug from the blood based on their position relative to the drug (Shelton et al., 2008). As a result, part of the drug is removed without using the body. The most important disadvantages of the old methods are drug wastage, dose-related side effects, high raw material costs, physicochemical incompatibilities, and clinical drug interactions (Shelton et al., 2008). In order to prevent and reduce these disadvantages, the new pharmaceutical industry took steps to produce and use new drug delivery systems (Zahin et al., 2019). The most important of these systems, which are widely researched today, are hydrogels, nanofibers, nanomicelles, and nanoliposomes (Aberoumandi et al., 2017). In modern drug formulation studies, small amounts of the active ingredient can be formulated into the nano-based platform to increase the bioavailability and potency of drugs and also reduce their unwanted side effects (Zahin et al., 2019; Aberoumandi et al., 2017). In the pharmaceutical systems, nanomicelles have become a highly studied nano-based drug delivery systems to improve drug efficiency (Aliabadi and Lavasanifar, 2006; Lu et al., 2018). The use of such structures due to their many similarities with biological membranes and also their targeting, in addition to improving the effectiveness of the drug, can also significantly reduce the side effects of drugs (Aliabadi and Lavasanifar, 2006; Lu et al., 2018).

Considering that a limited number of studies have done on the mechanism involved in the protective effects of calycosin in the form of free or nano-formulated state on Dox-induced cardiotoxicity, therefore, we aimed to explore the preventive characteristics of calycosin and calycosin-loaded nanomicelles on the complications of cardiotoxicity stimulated by Dox *in vitro*.

2. Materials and methods

2.1. Materials

Doxorubicin hydrochloride (Dox), Poly(ethylene glycol)-block-poly(propylene glycol)-block-poly(ethylene glycol) (PEG-PPG-PEG), 3-(4, 5-dimethyl-2-thiazolyl)-2, 5-diphenyl-2H-tetrazolium bromide (MTT), and 2, 7-dichlorodihydrofluorescein diacetate (H2-DCFDA) were purchased from Sigma-Aldrich (St Louis, MO, USA). RPMI-1640 and fetal bovine serum (FBS) was obtained from Gibco BRL (Grand Island, NY, USA).

3. Methods

3.1. Preparation of calycosin-loaded triblock copolymer nanomicelles

Calycosin-loaded PEG-PPG-PEG nanomicelles were prepared via dialysis approach. Briefly, calycosin (0.3 mg/ml) and the PEG-PPG-PEG copolymer (3 mg/ml) were hydrated in 100 ml of dioxane and the solution was mixed and stirred at 500 rpm for 50 min, followed by addition of 3 ml deionized (DI) water drop-wise for 60 min under constant stirring. The obtained micellar solution was then transferred into dialysis membrane (MWCO 700 g/mol) against DI water for 5 h. Empty PEG-PPG-PEG nanomicelles were also synthesized by the similar method in the absence of calycosin.

3.2. Characterization of the calycosin-loaded triblock copolymer nanomicelles

The hydrodynamic size, polydispersity and zeta-potential of prepared nanomicelles were explored using a Zetasizer analyzer (Malvern, UK). Samples were dispersed in DI water and analyzed at room temperature. The morphology of the nanomicelles was determined using transmission electron microscopy (TEM, Philips, CM-100, Germany). A drop of sample was dropped on the copper grid-carbon film and dried at room temperature. The critical micellar concentration (CMC) was determined by using 1,6-diphenyl-1,3,5-hexatriene (DPH) probe, which 25 ml DPH solubilized in methanol (0.5 mM), was mixed with micellar solution with different concentrations ranging from 0.001 to 0.5 mg/mL and the absorbance was read at 350 nm using UV-vis spectrophotometer (Beckman Coulter).

3.3. Encapsulation efficiency and calycosin content determination

Dialysis method (MWCO 700 g/mol) was used to determine the amount of calycosin encapsulation based on using UV-vis spectrophotometry at 428 nm (Beckman Coulter) using a standard calibration curve. The Dox loading capacity (LC) was determined as a difference between the initial concentration of calycosin and the concentration in the aqueous sample after the dialysis method. The encapsulation efficiency (EE) was calculated based on the following equation (Li et al., 2017):

$$EE(\%) = (\text{Total amount of calycosin} - \text{free calycosin}) / \text{Total amount of calycosin}.$$

3.4. *In vitro* release study

In vitro release of calycosin from the PEG-PPG-PEG nanomicelles was investigated in a PBS buffer (pH 7.4, 100 mM) at room temperature. The prepared micellar solution was poured into a dialysis bag (MW = 7000 g/mol) and immersed into 200 ml of PBS containing 2% ethanol under constant stirring (50 rpm) at 37 °C. At different time intervals, a defined amount of sample was withdrawn and replaced by fresh PBS buffer and the concentration of the released calycosin was quantified by UV-vis spectrophotometry as stated above.

3.5. Antioxidant activity of free and calycosin-loaded triblock copolymer nanomicelles

The antioxidant activity of free and micellar calycosin with a concentration of 0.1 mg/mL was explored by ABTS assay kit (CS0790, sigma, USA) and hypochlorite assay kit (2687100, Hach Co. USA) based on the manufacturer's protocols. The antioxidant activity of samples was estimated using the following equation:

Antioxidant activity = $(A_0 - A) / A_0$, where A_0 is the absorbance of the control and A is the absorbance of samples containing free calycosin or calycosin-loaded nanomicelles. Vitamin C with a concentration of 1 mg/mL was used as a positive control.

3.6. Cell culture

Cardiac muscle cells (H9C2 cells) were cultured in RPMI-1640 cell culture medium supplemented with FBS 10% (v/v) and 1% penicillin-streptomycin in a humidified atmosphere at 37 °C with 5% CO₂.

3.7. MTT assay

The cytotoxicity of the Dox, free calycosin, calycosin-loaded triblock copolymer nanomicelles, and empty triblock copolymer nanomicelles with different Dox or calycosin concentrations (0.01, 0.1, 1, 10, 20, 50 µg/mL) against H9C2 cells was determined by MTT assay. After 24 h incubation, 10 µL of MTT solution was added to each well and incubated for another 4 h, and then 200 µL of DMSO was added to the samples. The absorbance was then read at 570 nm using a microplate reader (BioRad, USA).

3.8. Measurement of intracellular ROS generation

The DCFH-DA assay was used (Alarifi et al., 2017) to determine the antioxidant effects of free calycosin or calycosin-loaded triblock copolymer nanomicelles against Dox-induced ROS production. The cells were exposed to a IC₅₀ concentration of Dox (a concentration of Dox inhibit the viability of cells by 50%), Dox and calycosin (10 µg/ml, the maximum dose with no cytotoxicity), Dox and calycosin-loaded triblock copolymer nanomicelles (10 µg/ml calycosin), and Dox and

triblock copolymer nanomicelles (equivalent concentration to 10 µg/ml calycosin). After incubation for 24 h, the cells were incubated with 10 µM DCFH-DA for 30 min and the fluorescence intensity of the samples was read using a fluorescence microplate reader (BioRad, USA) and the relevant images were taken by fluorescence microscopy (Zeiss, Germany).

3.9. Intracellular RNS measurement

The RNS level was assessed employing RNS Assay Kit (Best-Bio, China). Cells were washed, stained with BBoxiProbe™ R21F (10 µM) for 30 min, and washed again with PBS. Finally, RNS level was determined by using a fluorescence microplate reader (BioRad, USA).

3.10. Silencing ERp57 mRNA

ERp57-siRNA (5'-GGGCAAG GACUUACUUUU-3') was employed to silence the ERp57 mRNA based on a previous report (Li et al., 2019). Also, a random nucleotide sequence (5'-UUCUCCGAACGUGUCACGU-3') was employed as a negative control (NC) siRNA. Transfection of siRNA (50 nM) was done using Lipofectamine 2000 (Invitrogen, USA) based on the manufacturer's instruction and incubated for 48 h. Total mRNAs and proteins of the cells were then extracted and used for quantitative polymerase chain reaction (qPCR) and western blot assays, respectively.

3.11. qPCR assay

After treatment, the cells were collected, washed, total RNA was extracted (TRIzol reagent, Invitrogen; Thermo Fisher Scientific, Inc.) and cDNA was synthesized using a PrimeScript RT Reagent kit (Takara Bio, Japan). qPCR was carried out based on SYBR Premix Ex Taq II (Takara Bio, Japan) based on the manufacturer's instructions. Table 1 shows the primers were used in the present study. The qPCR assay was done with an ABI system (PRISM 7500; Thermo Fisher Scientific, Inc.) based on the 2^{-ΔΔC_t} method (Schmittgen and Livak, 2008).

3.12. Western blot analysis

The cells were transfected with ERp57-siRNA for 48 h, followed by addition of a single concentration of Dox (IC₅₀ concentration of Dox), Dox and calycosin (10 µg/ml, the maximum concentration with no cytotoxicity), Dox and calycosin-loaded triblock copolymer nanomicelles (10 µg/ml calycosin), and Dox and triblock copolymer nanomicelles (equivalent concentration to 5 µg/ml calycosin). Afterward, the western blot analysis was done based on the previous report (Huang et al., 2020). The following antibodies were used: Monoclonal anti-ERp57 (cat. no. sc80648, Santa Cruz, CA, USA), monoclonal anti-p53 (cat. no. WL01804, Wanlei Biotechnology, Shenyang, China), and monoclonal anti-GAPDH (cat. no.60004-1-Ig, ProteinTech Group Inc. Wuhan, China) and diluted to 1:1000 (Huang et al., 2020). The secondary antibodies (anti-mouse cat. no. ZB-2305; ZSGB-Bio, Beijing, China) were diluted to 1:10,000 and the signal was detected using a chemiluminescence kit (cat. no. WLA003a;

Table 1 Primer sequences for qPCR assay.

Primer	Forward	Reverse
ERp57	5'-GAGCAATGATGGGCC TGTGA-3'	5'-GGCATGGACTGTGGTCATGAG-3'
p53	5'-ACCTATGGAACTACTTCTGAAA-3'	5'-CTGGCATTCTGGGAGCTTCA-3'
Bax	5'-CAGGATGCGTCCACCAAGAA-3'	5'-CGTGTCCACGTCAGCAATCA-3'
Bcl-2	5'-GGATGCCTTTGTGGAAGTGT-3'	5'-AGCCTGCAGCTTTGTTTCAT-3'
GAPDH	5'-TGCACCACCAACTGCTT AGC-3'	5'-GGCATGGACTGTGGTCATGAG-3'

Wanlei Life Science, Shenyang, China) using a chemiluminescence detection system (Tanon-5200, Shanghai, China).

3.13. Statistical analysis

Student *t*-test was used to compare two sets of data and one-way analysis of variance followed by a post-hoc Tukey's test was used to compare multiple groups using SPSS version 22.0 (IBM SPSS, Armonk, NY, USA). Data are presented as means \pm standard deviation (SD) of three independent experiments. $P < 0.05$ was considered to show a statistically significant difference.

4. Results and discussion

4.1. Characterization of nanomicelle

DLS analysis for free PEG-PPG-PEG nanomicelles and calycosin-PEG-PPG-PEG nanomicelles showed hydrodynamic radii of about 73 ± 6.11 nm (PDI: 0.241) and

83.27 ± 7.21 (PDI: 0.268), respectively (Fig. 1A). It was observed a monomodal particle size distribution for both empty and loaded-nanomicelles with a slight difference in the size distribution. TEM image also demonstrated that the size of the spherical-shaped calycosin-PEG-PPG-PEG nanomicelles is about 20–30 nm (Fig. 1A, insert).

This data was also confirmed with the outcomes determined by zeta potential analysis (Fig. 1B). These data clearly showed that the zeta potential value of free PEG-PPG-PEG nanomicelles was about -21.9 ± 3.98 mV, which decreased to -17.8 ± 2.68 mV upon encapsulation of calycosin (Fig. 1B), indicating the successful loading of drugs into the nanomicelles.

To further assess the potential fabrication of calycosin-PEG-PPG-PEG, FTIR analysis was carried out. The FTIR spectra of calycosin, PEG-PPG-PEG and calycosin-PEG-PPG-PEG are shown in Fig. 1C. The peaks are located at 911 cm^{-1} , 1657 cm^{-1} , 1555 cm^{-1} , 1483 cm^{-1} , 1695 cm^{-1} , and 3309 cm^{-1} are characteristic vibrations of calycosin (Xie et al., 2018). The PEG-PPG-PEG peaks show the characteristic vibration of PEG and PPG (Lee et al., 2008). Afterwards, some common characteristic vibrations can be observed in

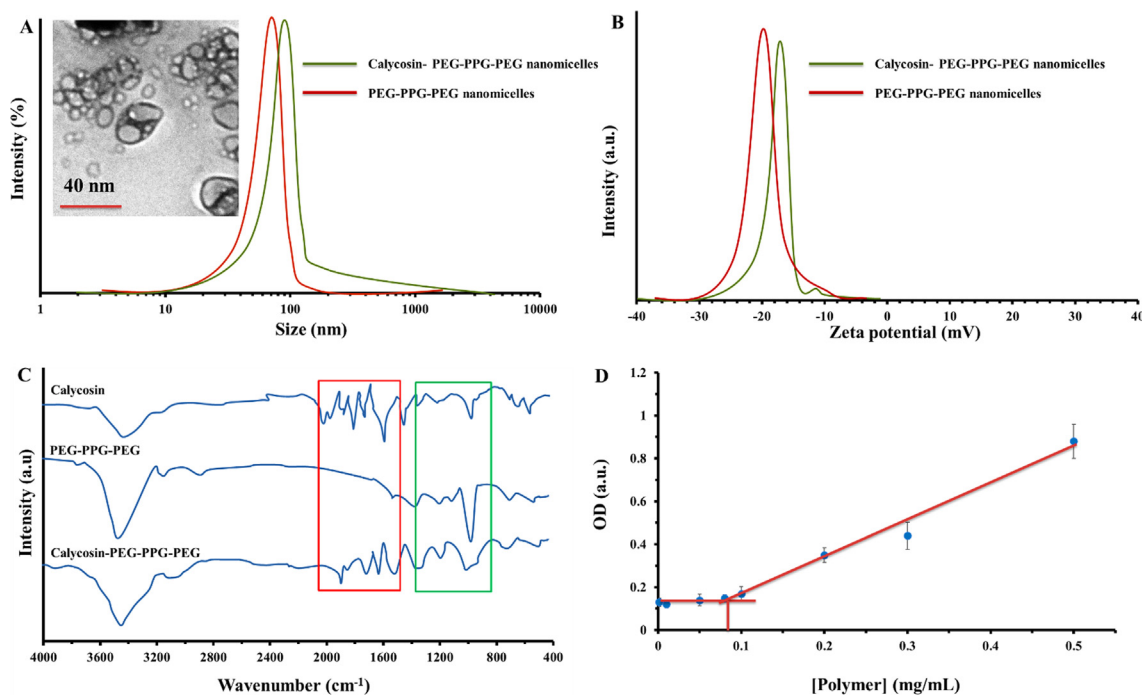


Fig. 1 (A) Particle size distribution of free and calycosin-PEG-PPG-PEG nanomicelles. The inset shows the TEM image of nanomicelles. (B) Zeta potential values of free and calycosin-PEG-PPG-PEG nanomicelles. (C) FTIR spectra of calycosin, PEG-PPG-PEG copolymer and calycosin-PEG-PPG-PEG compound. (D) CMC determination based on UV/vis spectroscopy. Data are presented as means \pm (SD) of three independent experiments.

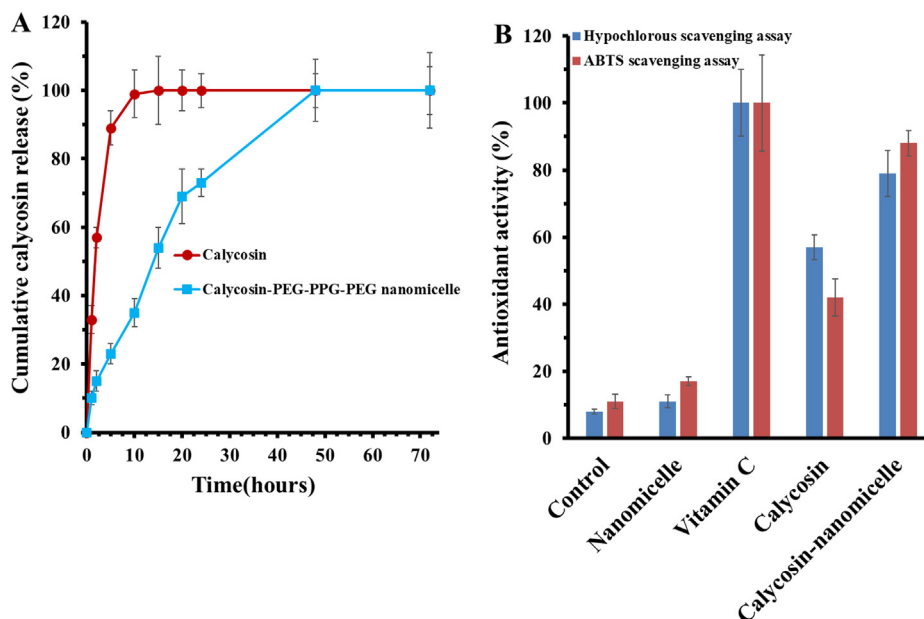


Fig. 2 (A) In vitro drug release profiles of free and calycosin-PEG-PPG-PEG nanomicelles in PBS (pH 7.4). (B) Antioxidant activity of free and calycosin-PEG-PPG-PEG nanomicelles determined by the relevant experiments. Data are presented as means \pm (SD) of three independent experiments.

calycosin-PEG-PPG-PEG bands, indicating the successful preparation of the drug-loaded nanomicelles.

The CMC of the PEG-PPG-PEG copolymer was determined based on the solubilization of DPH probe after interaction with hydrophobic micellar cores and corresponding absorbance changes at 390 nm. Fig. 1D shows the changes in the absorbance of PEG-PPG-PEG/DPH micellar dispersions at different copolymer concentrations. Based on Fig. 1D, the aggregation process was significantly observed above a concentration of 0.086 mg/mL.

It was also shown that DL% and EE% of calycosin-PEG-PPG-PEG nanomicelles were $7.38 \pm 1.15\%$ and $87.61 \pm 3.86\%$, respectively.

4.2. In vitro drug release and antioxidant activity studies

The *in vitro* release profile of calycosin from PEG-PPG-PEG nanomicelles was explored in a PBS buffer with pH of 7.4 (Fig. 2A). The outcome showed a sustained calycosin release in the PBS buffer with a weaker burst phase relative to free calycosin. The determined sustained calycosin release was potentially due to the hydrophobic forces between PPG micellar core and calycosin. Indeed, due to the instability of and calycosin at physiological conditions, the nano-formulation of calycosin into the nanomicelles could be a potential candidate for its stabilization. However, during the encapsulation phase, some degradation and inactivation of drugs can be induced. Therefore, the antioxidant activity of calycosin-PEG-PPG-PEG nanomicelles was explored to assess their function. Fig. 2B showed the antioxidant activity explored by ABTS radical and hypochlorous scavenging assays, respectively. As shown in Fig. 2B, the ability of the calycosin-PEG-PPG-PEG nanomicelles to neutralize the ABTS radical and hypochlorite ions was significantly greater than that of the free

calycosin. Therefore, the increased antioxidant activity of calycosin-PEG-PPG-PEG nanomicelles could be associated with the improved solubility of micellar drug in comparison with that of free drug.

4.3. MTT assay

To explore whether PEG-PPG-PEG nanomicelle enhanced the bioavailability of calycosin and reduced the cytotoxicity of calycosin in the H9C2 cells, their cytotoxic assay was done and compared (Fig. 3A). After treatment, the cells exhibited no significant reduction in viability up to the concentration of 10 $\mu\text{g}/\text{ml}$ and 50 $\mu\text{g}/\text{ml}$ for free calycosin and calycosin-PEG-PPG-PEG nanomicelles, respectively showing that nanomicelle formulation can reduce the cytotoxic effects of calycosin at high concentrations (Fig. 3A).

It was also observed that Dox induced cytotoxicity at extremely low concentrations starting from 0.01 $\mu\text{g}/\text{ml}$ (Fig. 3A) with an IC_{50} concentration (a concentration of Dox inhibit the viability of cells by 50%) of 0.19 $\mu\text{g}/\text{ml}$. Therefore, for further studies to induce cytotoxicity in H9C2 cells by Dox, its IC_{50} concentration was used and for the exploring the protective effects of free or nano-formulated calycosin the optimum concentration of calycosin with no significant cytotoxic effect (10 $\mu\text{g}/\text{ml}$) was used.

It was seen that the viability of the H9C2 cells was significantly decreased ($***P < 0.001$; $n = 3$) following incubation with Dox for 24 h compared with the negative control cells (Fig. 3B). By contrast, treatment of the H9C2 cells with free calycosin ($^{\#}P < 0.05$; $n = 3$) or calycosin-PEG-PPG-PEG nanomicelles ($^{\#\#}P < 0.01$; $n = 3$) caused increased cell survival, whereas, the inhibitory effect of nano-formulated calycosin was more significant than free drug ($*P < 0.05$; $n = 3$).

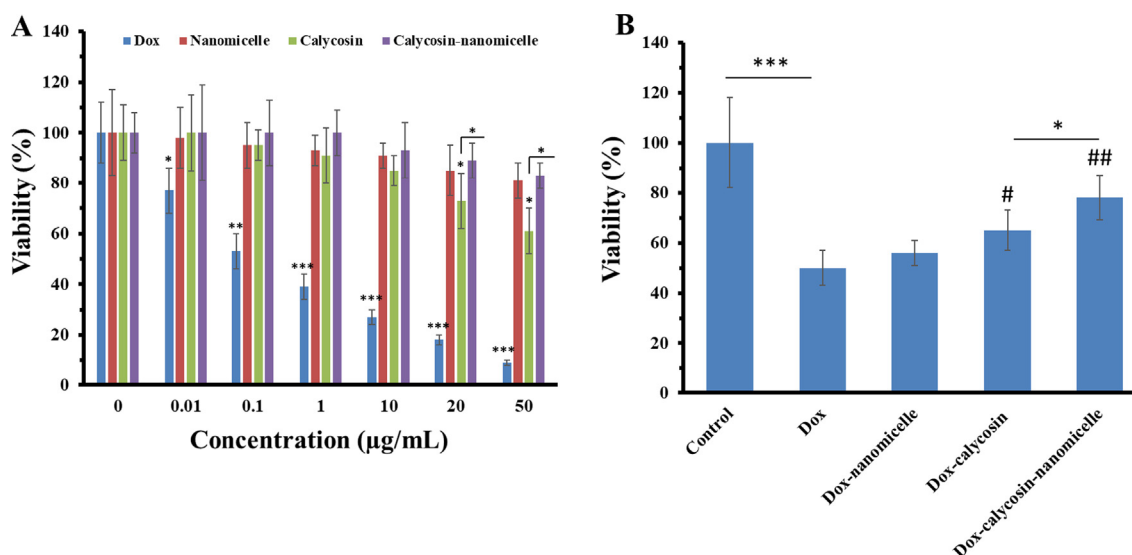


Fig. 3 (A) MTT assay of H9C2 cells incubated with different concentrations (0.01–50 µg/mL) of Dox, nanomicelles, free calycosin and calycosin-PEG-PPG-PEG nanomicelles for 24 h. (B) MTT assay of cells incubated with IC₅₀ concentration of Dox and the protective effects of co-incubation of calycosin (10 µg/mL) or calycosin-PEG-PPG-PEG nanomicelles (10 µg/mL) against Dox-induced cardiotoxicity. Data are presented as means ± (SD) of three independent experiments. **P* < 0.05, ***P* < 0.01, ****P* < 0.001: relative to control group; #*P* < 0.05, ##*P* < 0.01: relative to Dox-incubated cells.

4.4. Ros and RNS assays

To further explore the calycosin-nanomicelles protective effects, we investigated their effects on generation of intracellular ROS and RNS (Fig. 4). Quantitative measurements of the ROS (Fig. 4A) and RNS (Fig. 4B) indicated that Dox increased ROS and RNS generation in the H9C2 cells. The increase in the intracellular ROS and RNS was markedly inhibited with free calycosin or calycosin-PEG-PPG-PEG nanomicelles, whereas calycosin in the nano-formulated platform showed a greater protective effect (**P* < 0.05) against ROS and RNS generation induced by Dox in the H9C2 cells. Also, fluorescence imaging showed the number of bright green cells as a marker of ROS production was greatly decreased after treatment of cells with calycosin-PEG-PPG-PEG nanomicelles (Fig. 4C), which is in good agreement with the quantified DCF fluorescence intensity data.

4.5. qPCR assay

It has been well-documented that excessive ROS and RNS can stimulate apoptotic death through different signaling pathways. Therefore, we examined the relative expression of different mRNA, including ERp57, p53, Bax, and Bcl-2. It was shown that upon exposure of cells to Dox, a significant over-expression in the p53 and Bax mRNA was observed, whereas ERp57 and Bcl-2 mRNA were downregulated (****P* < 0.001; *n* = 3) (Fig. 5A). By contrast, treatment with calycosin or calycosin-nanomicelles regulated the expression of these genes, whereas the determined productive effects were more pronounced for nano-formulated drug than free one (**P* < 0.05) (Fig. 5A).

To more explore the signaling pathway involved in the protective effects of calycosin-PEG-PPG-PEG nanomicelles against Dox-induced cardiotoxicity in H9C2 cells, the expres-

sion levels of the selected genes were explored in cells treated with ERp57-siRNA and different treatments. As indicated in Fig. 5B, ERp57-siRNA silencing significantly downregulated the expression of ERp57 mRNA (****P* < 0.05), whereas, NC-siRNA did not significantly change the expression of this mRNA.

The effects of ERp57-siRNA silencing on Dox-induced cardiotoxicity and the protective effect of calycosin-PEG-PPG-PEG nanomicelles were examined using qPCR assay. The expression level of ERp57, p53, Bax, and Bcl-2 mRNA in the cells treated with ERp57 siRNA and Dox changed significantly (****P* < 0.001) in comparison with a negative control sample (Fig. 5C). Furthermore, the ERp57 siRNA/Dox-treated cells incubated with calycosin-PEG-PPG-PEG nanomicelles did not show any regulation in the expressing level of mRNA, indicating that silencing ERp57 mRNA has inhibited the protective effect of calycosin-PEG-PPG-PEG nanomicelles.

4.6. Western blot analysis

The regulation of the selected proteins was determined in cells incubated with ERp57-siRNA, Dox and calycosin-PEG-PPG-PEG nanomicelles. As indicated in Fig. 6, when H9C2 cells were treated with Dox, protein expression was significantly changed relative to negative control cells, which was almost regulated in the presence of calycosin-nanomicelles. However, once ERp57-siRNA was applied, expression levels of protein were greatly influenced, which suggested that treatment of ERp57-siRNA outstandingly prohibited the protective effects of calycosin-nanomicelles and increased protein de-regulation induced by Dox. Indeed, the expression levels of ERp57 and Bcl-2 were reduced and those of p53 and Bax were significantly increased in response to Dox. When the cells were incubated with Dox and

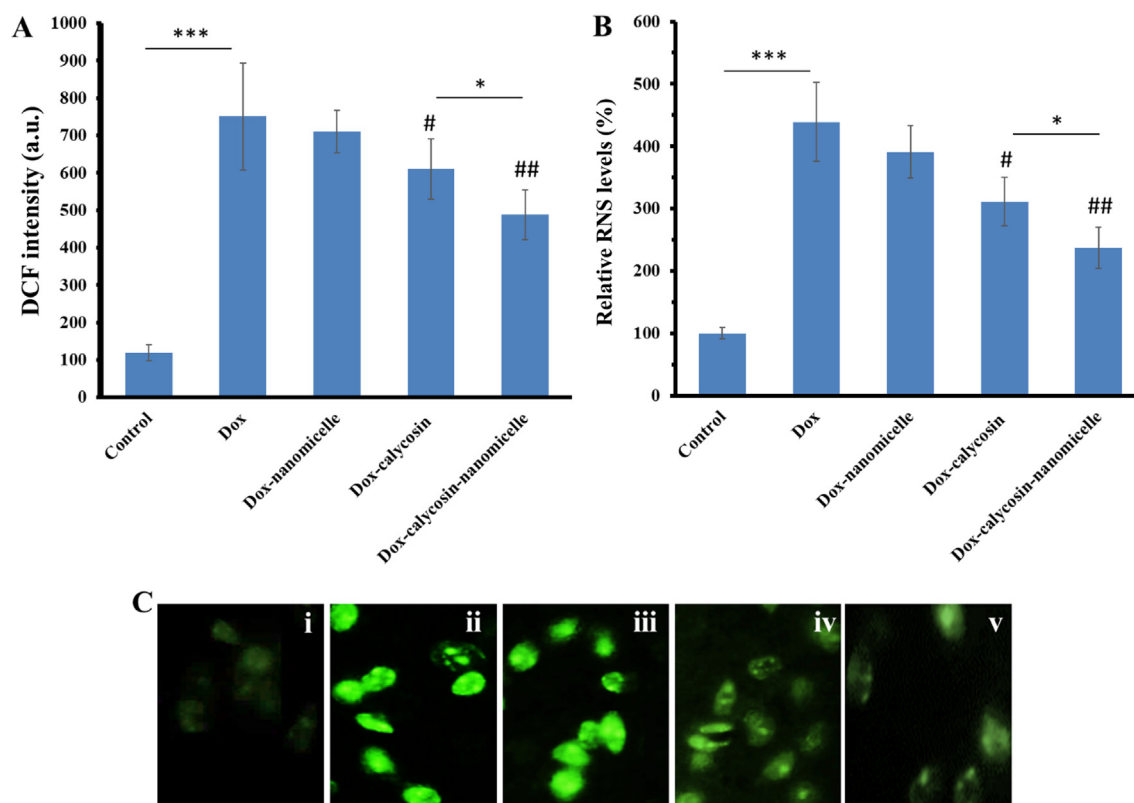


Fig. 4 (A) ROS and (B) RNS assays of H9C2 cells incubated with IC_{50} concentration of Dox and the protective effects of co-incubation of calycosin ($10 \mu\text{g/mL}$) or calycosin-PEG-PPG-PEG nanomicelles ($10 \mu\text{g/mL}$) against Dox-induced ROS and RNS production. (C) ROS assay determined by fluorescence microscopy (i: control, ii: Dox-incubated cell, iii: Dox-nanomicelles-incubated cells, iv: Dox-calycosin-incubated cells, v: Dox-calycosin-nanomicelles-incubated cells). Data are presented as means \pm (SD) of three independent experiments. * $P < 0.05$, ** $P < 0.01$, *** $P < 0.001$: relative to control group; # $P < 0.05$, ## $P < 0.01$: relative to Dox-incubated cells.

calycosin-nanomicelles, the expression levels of these proteins were almost regulated. However, ERp57 siRNA silencing restored the upregulation of Bax and p53 proteins and down-regulation of ERp57 and Bcl-2 proteins of cells. In general in agreement with qPCR assay, western blot analysis indicated that co-incubation of cells with ERp57-siRNA, Dox and calycosin-PEG-PPG-PEG nanomicelles reduced the protective effect of calycosin.

It has been shown that calycosin results in the mitigation of myocardial injury (Tsai et al., 2019; Liu et al., 2020) and recovery of heart function (Huang et al., 2020). It has been also shown that calycosin leads to cardiovascular protective effects (Li et al., 2020) mediated by estrogen receptor- α/β (Liu et al., 2016). Also, it has been reported that calycosin mitigated Dox-stimulated cardiotoxicity by inhibiting oxidative stress and inflammatory responses through sirtuin 1 pathway (Zhai et al., 2020). Based on the unique characteristics of polyphenol compounds (unwanted side effects and low solubility at high concentration), different formulation strategies have been proposed to increase their bioavailability and pharmaceutical potency (Salehi et al., 2020; Jain et al., 2015; Conte et al., 2016). PEG and PPG polymers due to their biocompatible structures and unique physicochemical properties have been widely used for preparation of self-assembled nanomicelles for hydrophobic drug delivery (Gong et al.,

2010; Öcal et al., 2014; Kim et al., 2017). In the present work, we found that nano-formulation of calycosin results in improvement of its protective effects against Dox-induced cardiotoxicity *in vitro*.

ERp57 as a thiol oxidoreductase of the endoplasmic reticulum is widely expressed with variable levels within different tissues. Several studies have reported the diverse well-defined activities of ERp57 in different diseases. De-expression of ERp57 has been associated with different disease from cancer to neurodegenerative disorders (Hettinghouse et al., 2018). Also, it has been reported that ERp57 can be implemented as a target for some drugs as cardioprotective agents (Cui et al., 2015).

Therefore, this paper was aimed to provide some information related to regulation of ERp57 in Dox-induced cardiotoxicity and the protective effect of calycosin-loaded nanomicelles, which highlights the potential biomedical applications of targeting ERp57.

Therefore, this paper may provide a model to express the biological effect of ERp57 in Dox-induced cardiotoxicity and the side effects and limitations reversal of Dox by calycosin either alone or in the nano-formulated platform. The data indicated that Dox treatment of H9C2 cells leads to low ERp57 expression. As a result, calycosin treatment in the both forms of free and nano-formulated species can activate the

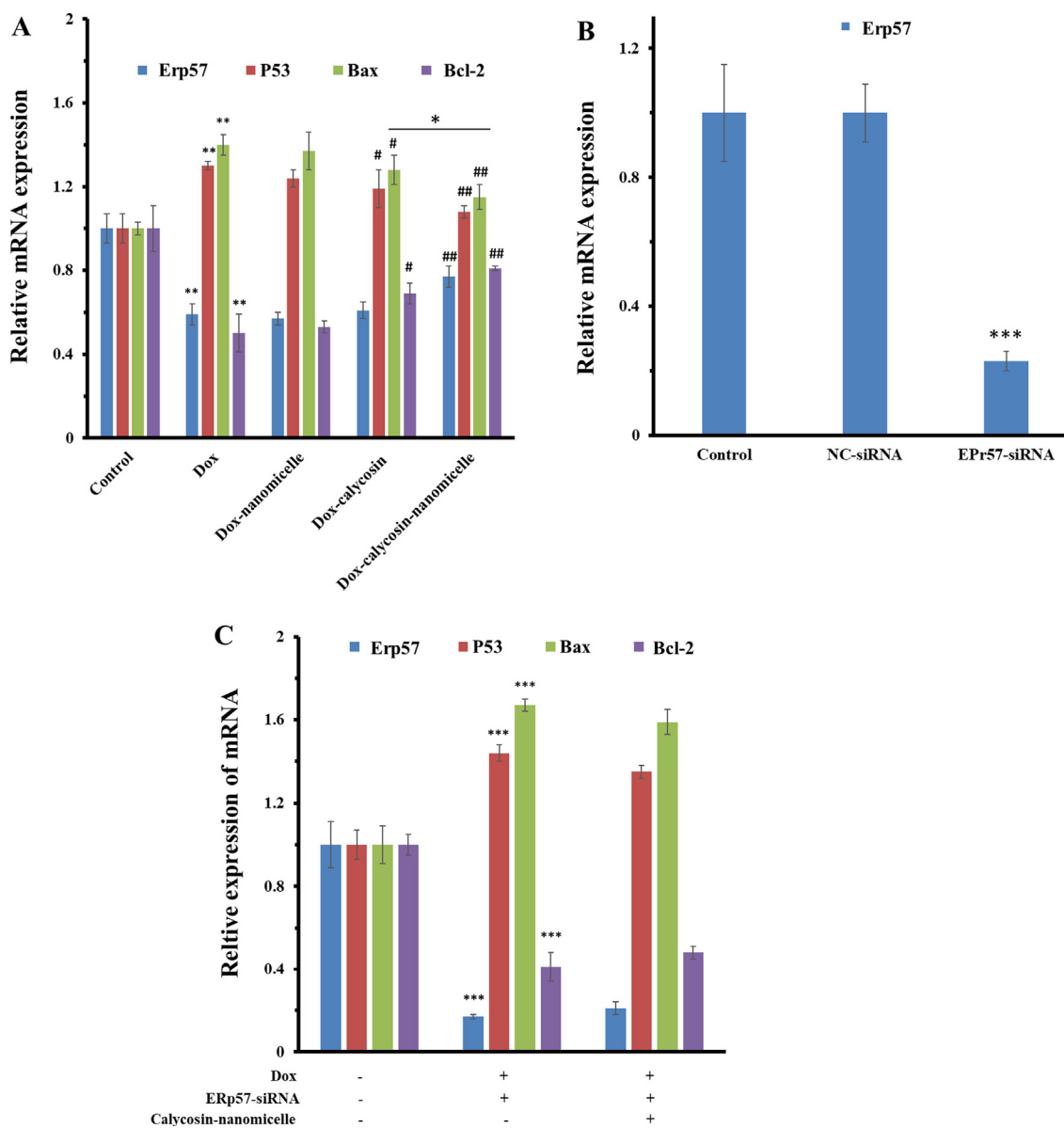


Fig. 5 (A) qPCR assay of H9C2 cells incubated with IC₅₀ concentration of Dox and the protective effects of co-incubation of calycosin (10 $\mu\text{g}/\text{mL}$) or calycosin-PEG-PPG-PEG nanomicelles (10 $\mu\text{g}/\text{mL}$) against Dox-induced ERp57, Bcl-2/p53, Bax downregulation/upregulation. (B) qPCR assay of the ERp57 mRNA expression levels of H9C2 cells incubated with blank, NC-siRNA and ERp57-siRNA. (C) Relative expression of ERp57, p53, Bax, and Bcl-2 mRNA in the presence of Dox and ERp57 siRNA. Data are presented as means \pm (SD) of three independent experiments. * $P < 0.05$, ** $P < 0.01$, *** $P < 0.001$: relative to control group; # $P < 0.05$, ## $P < 0.01$: relative to Dox-incubated cells.

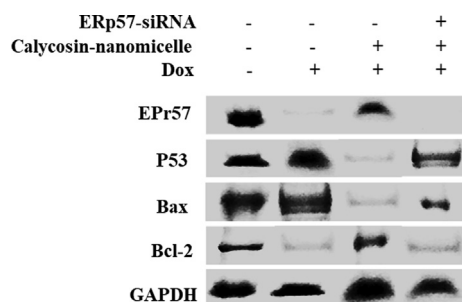


Fig. 6 Western blot analyses of ERp57, p53, Bax, and Bcl-2 proteins of H9C2 cells under different treatments. GAPDH was used as the internal standard.

ERp57 signaling pathway, which mitigates the apoptosis process. The outcomes of this study may provide useful information to overcome the cardiotoxicity challenge in the clinical treatment of different cancers.

5. Conclusion

In the present study PEG-PPG-PEG copolymer nanomicelles with a size of 20–30 nm were prepared and the potential drug loading, colloidal stability and sustained drug release were determined by relevant assays. Moreover, it was indicated that calycosin-PEG-PPG-PEG nanomicelles can reduce Dox-induced cardiotoxicity through ERp57

signaling pathway. Therefore, this report can hold a great promise for development of drug-loaded nanostructures for mitigation of Dox-triggered cytotoxicity.

Declaration of Competing Interest

The authors declare that they have no known competing financial interests or personal relationships that could have appeared to influence the work reported in this paper.

Acknowledgment

None.

References

- Tacar, O., Sriamornsak, P., Dass, C.R., 2013. Doxorubicin: an update on anticancer molecular action, toxicity and novel drug delivery systems. *J. Pharm. Pharmacol.* 65 (2), 157–170.
- Hayward, R., Hydock, D., Gibson, N., Greufe, S., Bredahl, E., Parry, T., 2013. Tissue retention of doxorubicin and its effects on cardiac, smooth, and skeletal muscle function. *J. Physiol. Biochem.* 69 (2), 177–187.
- Kalyanaraman, B.J.S.S.E.S., Joseph, J., Kalivendi, S., Wang, S., Konorev, E., Kotamraju, S., 2002. Doxorubicin-induced apoptosis: implications in cardiotoxicity. *Mol. Cell. Biochem.* 234 (1), 119–124.
- Deres, P., Halmosi, R., Toth, A., Kovacs, K., Palfi, A., Habon, T., Czopf, L., Kalai, T., Hideg, K., Sumegi, B., Toth, K., 2005. Prevention of doxorubicin-induced acute cardiotoxicity by an experimental antioxidant compound. *J. Cardiovasc. Pharmacol.* 45 (1), 36–43.
- Jones, P.A., Laird, P.W., 1999 Feb. Cancer-epigenetics comes of age. *Nat. Genet.* 21 (2), 163–167.
- Zilinyi, R., Czompa, A., Czegledi, A., Gajtko, A., Pituk, D., Lekli, I., Tosaki, A., 2018 May. The cardioprotective effect of metformin in doxorubicin-induced cardiotoxicity: the role of autophagy. *Molecules* 23 (5), 1184.
- Ascensão, A., Magalhães, J., Soares, J., Ferreira, R., Neuparth, M., Marques, F., Duarte, J., 2006. Endurance exercise training attenuates morphological signs of cardiac muscle damage induced by doxorubicin in male mice. *Basic Appl. Myol.* 16 (1), 27–35.
- McCord, J.M., 1986 Jan 1. Superoxide dismutase: rationale for use in reperfusion injury and inflammation. *J. Free Radicals Biol. Med.* 2 (5–6), 307–310.
- Bernier, M., Hearse, D.J., Manning, A.S., 1986 Mar. Reperfusion-induced arrhythmias and oxygen-derived free radicals. Studies with “anti-free radical” interventions and a free radical-generating system in the isolated perfused rat heart. *Circ. Res.* 58 (3), 331–340.
- Martin, J., Lutter, G., Sarai, K., Senn-Grossberger, M., Takahashi, N., Bitu-Moreno, J., Haberstroh, J., Beyersdorf, F., 2001 Mar 1. Investigations on the new free radical scavenger polynitroxyl-albumin to prevent ischemia and reperfusion injury after orthotopic heart transplantation in the pig model. *Eur. J. Cardiothorac. Surg.* 19 (3), 321–325.
- Hearse, D.J., Tosaki, A., 1987 Mar. Free radicals and reperfusion-induced arrhythmias: protection by spin trap agent PBN in the rat heart. *Circ. Res.* 60 (3), 375–383.
- Tosaki, A., Braquet, P., 1990 Oct 1. DMPO and reperfusion injury: arrhythmia, heart function, electron spin resonance, and nuclear magnetic resonance studies in isolated working guinea pig hearts. *Am. Heart J.* 120 (4), 819–830.
- Najafi, M., Ghavimi, H., Gharakhani, A., Garjani, A., 2015 Dec 13. Effects of hydroalcoholic extract of *Cynodon dactylon* (L.) pers. on ischemia/reperfusion-induced arrhythmias. *DARU J. Pharm. Sci.* 16 (4), 233–238.
- Bak, I., Lekli, I., Juhasz, B., Nagy, N., Varga, E., Varadi, J., Gesztelyi, R., Szabo, G., Szendrei, L., Bacskay, I., Vecsernyes, M., 2006 Sep. Cardioprotective mechanisms of *Prunus cerasus* (sour cherry) seed extract against ischemia-reperfusion-induced damage in isolated rat hearts. *Am. J. Physiol.-Heart Circulatory Physiol.* 291 (3), H1329–H1336.
- Haines, D.D., Juhasz, B., Tosaki, A., 2013 Aug. Management of multicellular senescence and oxidative stress. *J. Cell Mol. Med.* 17 (8), 936–957.
- Koleini, N., Kardami, E., 2017 Jul 11. Autophagy and mitophagy in the context of doxorubicin-induced cardiotoxicity. *Oncotarget.* 8 (28), 46663.
- Prathumsap, N., Shinlapawittayatorn, K., Chattipakorn, S.C., Chattipakorn, N., 2020 Jan. Effects of doxorubicin on the heart: From molecular mechanisms to intervention strategies. *Eur. J. Pharmacol.* 5 (866), 172818.
- Gao, J., Liu, Z.J., Chen, T., Zhao, D., 2014. Pharmaceutical properties of calycosin, the major bioactive isoflavonoid in the dry root extract of *Radix astragalii*. *Pharm. Biol.* 52 (9), 1217–1222.
- Tsai, C.C., Wu, H.H., Chang, C.P., Lin, C.H., Yang, H.H., 2019. Calycosin-7-O- β -D-glucoside reduces myocardial injury in heat stroke rats. *J. Formos. Med. Assoc.* 118 (3), 730–738.
- Liu, Y., Che, G., Di, Z., Sun, W., Tian, J., Ren, M., 2020. Calycosin-7-O- β -d-glucoside attenuates myocardial ischemia-reperfusion injury by activating JAK2/STAT3 signaling pathway via the regulation of IL-10 secretion in mice. *Mol. Cell. Biochem.* 463 (1), 175–187.
- Huang, J., Shen, H., Jiang, M., Huang, L., Yuan, Y. and Wang, Q., 2020. Calycosin reduces infarct size, oxidative stress and preserve heart function in isoproterenol-induced myocardial infarction model. *Pakistan J. Pharm. Sci.*, 33,5(2), 1-10.
- Li, P.A.N., Zhang, X.F., Wan-Sheng, W.E.I., Zhang, J., Zhen-Zhen, L.I., 2020. The cardiovascular protective effect and mechanism of calycosin and its derivatives. *Chinese J. Natural Med.* 18 (12), 27–35.
- Liu, B., Zhang, J., Liu, W., Liu, N., Fu, X., Kwan, H., Liu, S., Liu, B., Zhang, S., Yu, Z., Liu, S., 2016. Calycosin inhibits oxidative stress-induced cardiomyocyte apoptosis via activating estrogen receptor- α/β . *Bioorg. Med. Chem. Lett.* 26 (1), 181–185.
- Deng, M., Chen, H., Long, J., Song, J., Xie, L., Li, X., 2020. Calycosin: a review of its pharmacological effects and application prospects. *Expert Rev. Anti-infective Therapy*, 1–15.
- Shelton, B.M., Lebel, R.J. and Villegas, D.H., Infusion Systems LLC, 2008. Method and apparatus for automatically modifying delivery profile of drug delivery system. U.S. Patent 7,347,854.
- Zahin, N., Anwar, R., Tewari, D., Kabir, M.T., Sajid, A., Mathew, B., Uddin, M.S., Aleya, L., Abdel-Daim, M.M., 2019. Nanoparticles and its biomedical applications in health and diseases: special focus on drug delivery. *Environ. Sci. Pollut. Res.*, 1–18
- Aberoumandi, S.M., Mohammadhosseini, M., Abasi, E., Saghati, S., Nikzamir, N., Akbarzadeh, A., Panahi, Y., Davaran, S., 2017. An update on applications of nanostructured drug delivery systems in cancer therapy: a review. *Artif. Cells Nanomed. Biotechnol.* 45 (6), 1058–1068.
- Aliabadi, H.M., Lavasanifar, A., 2006. Polymeric micelles for drug delivery. *Expert Opin. Drug Deliv.* 3 (1), 139–162.
- Lu, Y., Yue, Z., Xie, J., Wang, W., Zhu, H., Zhang, E., Cao, Z., 2018. Micelles with ultralow critical micelle concentration as carriers for drug delivery. *Nat. Biomed. Eng.* 2 (5), 318–325.
- Li, J., Deng, J., Yuan, J., Fu, J., Li, X., Tong, A., Wang, Y., Chen, Y., Guo, G., 2017. Zonisamide-loaded triblock copolymer nanomicelles as a novel drug delivery system for the treatment of acute spinal cord injury. *Int. J. Nanomed.* 12, 2443–2450.
- Alarif, S., Ali, D., Alkahtani, S., Almeer, R.S., 2017 Jan. ROS-mediated apoptosis and genotoxicity induced by palladium nanoparticles in human skin malignant melanoma cells. *Oxid. Med. Cell. Longevity* 1, 2017.
- Li, S., Zhao, X., Chang, S., Li, Y., Guo, M., Guan, Y., 2019. ERp57–small interfering RNA silencing can enhance the sensitivity of

- drug-resistant human ovarian cancer cells to paclitaxel. *Int. J. Oncol.* 54 (1), 249–260.
- Schmittgen, T.D., Livak, K.J., 2008. Analyzing real-time PCR data by the comparative C_T method. *Nat. Protoc.* 3 (6), 1101.
- Xie, J., Xiong, J., Ding, L.S., Chen, L., Zhou, H., Liu, L., Zhang, Z.F., Hu, X.M., Luo, P., Qing, L.S., 2018. A efficient method to identify cardioprotective components of Astragali Radix using a combination of molecularly imprinted polymers-based knockout extract and activity evaluation. *J. Chromatogr. A* 1576, 10–18.
- Lee, J., Yang, J., Seo, S.B., Ko, H.J., Suh, J.S., Huh, Y.M., Haam, S., 2008. Smart nanoprobe for ultrasensitive detection of breast cancer via magnetic resonance imaging. *Nanotechnology* 19 (48), 485101.
- Zhai, J., Tao, L., Zhang, S., Gao, H., Zhang, Y., Sun, J., Song, Y., Qu, X., 2020. Calycosin ameliorates doxorubicin-induced cardiotoxicity by suppressing oxidative stress and inflammation via the sirtuin 1–NOD-like receptor protein 3 pathway. *Phytother. Res.* 34 (3), 649–659.
- Salehi, B., Prado-Audelo, D., María, L., Cortés, H., Leyva-Gómez, G., Stojanović-Radić, Z., Singh, Y.D., Patra, J.K., Das, G., Martins, N., Martorell, M., 2020. Therapeutic applications of curcumin nanomedicine formulations in cardiovascular diseases. *J. Clin. Med.* 9 (3), 746–750.
- Jain, A., Kesharwani, P., Kumar Garg, N., Jain, A., Nirbhavane, P., Dwivedi, N., Banerjee, S., K Iyer, A., Cairul Iqbal Mohd Amin, M., 2015. Nano-constructed carriers loaded with antioxidant: Boon for cardiovascular system. *Curr. Pharm. Des.*, 21(30), 4456–4464.
- Conte, R., Calarco, A., Napoletano, A., Valentino, A., Margarucci, S., Di Cristo, F., Di Salle, A., Peluso, G., 2016. Polyphenols nanoencapsulation for therapeutic applications. *J. Biomol. Res. Ther.* 5 (2), 1–10.
- Gong, C., Wei, X., Wang, X., Wang, Y., Guo, G., Mao, Y., Luo, F., Qian, Z., 2010. Biodegradable self-assembled PEG–PCL–PEG micelles for hydrophobic honokiol delivery: I. Preparation and characterization. *Nanotechnology* 21 (21), 215103–215110.
- Öcal, H., Arica-Yegin, B., Vural, İ., Goracinova, K., Çalış, S., 2014. 5-Fluorouracil-loaded PLA/PLGA PEG–PPG–PEG polymeric nanoparticles: formulation, in vitro characterization and cell culture studies. *Drug Dev. Ind. Pharm.* 40 (4), 560–567.
- Kim, H.A., Lee, H.J., Hong, J.H., Moon, H.J., Ko, D.Y., Jeong, B., 2017. α , ω -Diphenylalanine-end-capping of PEG-PPG-PEG polymers changes the micelle morphology and enhances stability of the thermogel. *Biomacromolecules* 18 (7), 2214–2219.
- Hettinghouse, A., Liu, R., Liu, C.J., 2018 Jan. Multifunctional molecule ERp57: from cancer to neurodegenerative diseases. *Pharmacol. Ther.* 1 (181), 34–48.
- Cui, G., Shan, L., Chu, I.K., Li, G., Leung, G.P., Wang, Y., Kwan, Y. W., Chan, S.W., Hoi, M.P., Lee, S.M., 2015. Identification of disulfide isomerase ERp57 as a target for small molecule cardioprotective agents. *RSC Adv.* 5 (91), 74605–74610.